Australasian Physical & Engineering Sciences in Medicine (2019) 42:677–688
https://doi.org/10.1007/s13246-019-00765-2

SCIENTIFIC PAPER

# Particle swarm optimization based fusion of ultrasound echographic and elastographic texture features for improved breast cancer detection

**S. Sasikala[1] · M. Bharathi[1] · M. Ezhilarasi[1] · Sathiya Senthil[2] · M. Ramasubba Reddy[3]**

Received: 11 June 2018 / Accepted: 23 May 2019 / Published online: 3 June 2019


**Abstract**
Breast cancer remains the main cause of cancer deaths among women in the world. As per the statistics, it is the most common killer disease of the new era. Since 2008, breast cancer incidences have increased by more than 20%, while mortality has increased by 14%. The statistics of breast cancer incidences as per GLOBOCAN project for the years 2008 and 2012 show an increase from 22.2 to 27% globally. In India, breast cancer accounts for 25% to 31% of all cancers in women. Mammography and Sonography are the two common imaging techniques used for the diagnosis and detection of breast cancer. Since Mammography fails to spot many cancers in the dense breast tissue of young patients, Sonography is preferred as an adjunct to Mammography to identify, characterize and localize breast lesions. This work aims to improve the performance of breast cancer detection by fusing the texture features from ultrasound elastographic and echographic images through Particle Swarm Optimization. The mean classification accuracy of Optimum Path Forest Classifier is used as an objective function in PSO. Seven performance metrics were computed to study the performance of the proposed technique using GLCM, GLDM, LAWs and LBP texture features through Support Vector Machine classifier. LBP feature provides accuracy, sensitivity, specificity, precision, F1 score, Mathews Correlation Coefficient and Balanced Classification Rate as 96.2%, 94.4%, 97.4%, 96.2%, 95.29%, 0.921, 95.88% respectively. The obtained performance using LBP feature is better compared to the other three features. An improvement of 6.18% in accuracy and 11.19% in specificity were achieved when compared to those obtained with previous works.

**Keywords** Breast cancer · Echography · Elastography · Feature fusion · Particle swarm optimization · Optimum path forest classifier · Support vector machine

## Introduction

To reduce the breast cancer fatality, early and accurate diagnosis is essential. Computer Aided Diagnosis (CADx) using Ultrasound (US) can be used as a second hand to assist physicians in diagnosing the tumour as benign or malignant accurately. As US imaging is portable, low cost and low risk to patients, it is extensively used in breast cancer diagnosis as a complementary tool to Mammography. B mode US or echographic imaging provides composite properties of tissues by capturing the characteristics of backscattered ultrasonic waves. Tumours possessing insufficient echographic properties provide inadequate details in B mode US image. US Strain Elastography (SE) mode image describes tissue stiffness and hardness in terms of spatial variations of the elastic modulus. It supplements useful and additional information about tumours for diagnosis.

✉ S. Sasikala
sundarsasi@gmail.com; sasikala.s.ece@kct.ac.in

M. Bharathi
bharathi.m.ece@kct.ac.in

M. Ezhilarasi
ezhilarasimuthusamy@gmail.com

Sathiya Senthil
senthilsathya@hotmail.com

M. Ramasubba Reddy
rsreddy@iitm.ac.in

[1] Kumaraguru College of Technology, Coimbatore, India

[2] Sonoscan Centre, Coimbatore, India

[3] Indian Institute of Technology Madras, Chennai, India

Many researchers have reported that SE mode do not have the potential to replace conventional B mode for the detection and diagnosis of breast cancer. However, it may be used as a supplement to B mode for improving the diagnostic performance. Many US machines have provisions to obtain B mode and SE mode images as paired images by simply changing appropriate probes. Many prospective studies proved that better diagnostic performance could be obtained by combining the information from these two images.

The performance of Real-time Tissue Elastography (RTE) was evaluated prospectively for breast mass detection. RTE and BIRADS evaluations were correlated with pathologic results. Pathologic examination detected 61 of 188 malignancies and 127 of 188 benign lesions (67.6%) correctly. The sensitivity and specificity obtained through RTE were 92.7% and 85.8% respectively. The authors confirmed that the use of RTE improves specificity, particularly for low-suspicion lesions [1]. Leong et al. evaluated 110 breast lesions against their histopathology reference standard with the help of seven dedicated breast radiologists. Their assessment was based on the BIRADS classification for Ultrasound B mode. The elastographic assessment was performed based on strain pattern and the elastographic size ratios. Their study showed that the sensitivity, specificity and accuracy as 88.5, 42.9 and 53.6% with conventional US, 100, 73.8, and 80% with elastography and 88.5, 78.6 and 80.9% with combined US and elastography respectively [2].

B mode US and elastography assessments were performed for 315 breast masses against histopathologic results. Two radiologists retrospectively evaluated the B mode images through BIRADS and elastographic images by the elasticity scoring and strain ratio. Areas under the ROCs were 0.616 for B mode US, 0.784 for elasticity score, 0.668 for strain ratio, 0.727 for the combination of B mode US and elasticity score and 0.701 for the combination of B mode US, elasticity score and strain ratio. The sensitivity, specificity, positive predictive value and negative predictive value were obtained as 93.8, 51.7, 25.9 and 97.9% respectively with elasticity score and B mode US combined [3].

A total of 308 breast tumours less than 2 cm in size were analyzed with both conventional US and US elastography and compared with pathological results. The sensitivities obtained with B mode and elastography were similar. When the two modalities have been combined together, the sensitivity was improved to 97.1%. Thus, it was reported that the US elastography in combination with B mode US improved the sensitivity of small breast tumours detection [4].

Healthy and metastatic axillary Lymph Nodes (LNs) of breast cancer patients were examined with palpation, US B mode, EI and Doppler. With respect to elasticity distribution, there was no difference in the cortex of medulla. But, cortexes in metastatic LNs were significantly harder than that in healthy LNs. Thus, elastography is capable of differentiating metastatic and healthy LNs and can improve the diagnostic performance. The sensitivity achieved with B mode, Doppler and EI were 13.3, 14.3 and 60.0% respectively and specificity values were 88.4, 96.8, 95.6 and 79.6% respectively. The highest specificities of 73.3% and 99.3% were achieved with the disjunctive and conjunctive combination of B mode and EI features respectively [5].

The breast cancer diagnostic performance of Strain Elastography (SE) and SWE individually combined with B mode US were compared through subjective assessment by two radiologists. No significant difference in the AUC was noted but an improved performance was noted for the combined sets (SE & B mode or SWE & B mode) [6].

Performance of BIRADS and BIRADS combined with SE were studied retrospectively for different size groups, age groups and area groups. 1194 breast lesions from 1080 patients were examined by conventional US and SE prior to Ultrasound-guided core biopsy. The accuracy of combined BIRADS and SE was improved by 13.2% for all lesions, 23.2% for $<10$ mm lesions, 13.3% for $\geq 10$–20 mm lesions, 6.3% for $\geq 20$ mm lesions, 18.4% for $<50$ age group and 1.7% for $\geq 50$ age group compared to the examination with BIRADS alone [7].

CAD based schemes for the detection of breast cancer using echographic or elastographic texture features separately were discussed in some literature. Few papers addressed the use of both echographic and elastographic texture features. In many works, the performance of the system using accuracy, sensitivity and specificity values were analyzed. In some literatures, any one of these three metrics was used. These metrics are not sufficient if there is any class imbalance in the data. The results of the CAD systems based on both echographic and elastographic features were discussed elaborately in discussion section and were compared with the results obtained through the proposed scheme of detection. Previous works shows a maximum specificity of 87.6%. This paper presents a new method to improve the performance particularly the specificity of the breast cancer detection based on the fusion of echographic and elastographic texture features, so that the number of false positives gets reduced.

## Materials and methods

### Dataset

The ultrasound elastographic and echographic images were collected from Sonoscan centre, Coimbatore during 2012 October to 2016 April using the Machine: Epiq 5G Ultrasound systems of Model: Epiq 5G1/SS with Make: Philips and a data set is formed. In Sonoscan centre, they are following a regular practice to get a consent from the patient (or

their family), to use the information for some retrospective studies after removing their identification information such as name and address that are not essential for the study. The same procedure was followed for the patients with breast disease also. The machine details and the procedure for getting patient consent are included as additional information at the end of this manuscript. Data set contains 113 cases, among which 62 are benign and 51 are malignant cases.

## Block diagram

The block diagram of the proposed system based on the fusion of both US B mode and SE mode image features is given in Fig. 1. In this system, US B mode and SE mode images are separately collected for both cancerous and non cancerous patients. Then, they are pre-processed individually to remove speckle noise and segmented to isolate the tumour regions. Then texture features are computed from both images separately and fused in serial fashion Particle swarm Optimization (PSO). Then, SVM is used to classify the features of US B mode and SE mode images individually and also the features after fusion. From the classification results, the performance measures are calculated.

## Preprocessing and segmentation

Ultrasound images usually contain speckle noise. Speckle Reducing Anisotropic Diffusion (SRAD) is used for speckle reduction in both B mode and E mode images. SRAD is a Partial Differential Equation (PDE) based edge-sensitive diffusion approach [8] which can remove speckle noise without distorting useful image information and without destroying the edges. In addition to preserving edges, SRAD can also enhance the edges by reducing diffusion across edges and allowing diffusion on either side of an edge. It is an adaptive method which does not employ hard thresholds to alter performance in homogeneous regions or in regions near edges and small features.

After speckle reduction, the tumour regions from the two images are segmented by a Fuzzy Level Set (FLS) algorithm proposed by Li et al. which employs a FCM clustering with some spatial restrictions to determine the approximate contours of interest in an image and its results are used to initiate automatic level set segmentation by estimating controlling parameters and regularizing level set evolution. Thus, initialization and parameter configuration of level set algorithm was automatized by spatial fuzzy clustering. The level set function was enhanced such that it can accommodate FCM results directly for evolution. Because, spatial fuzzy clustering combines the intensity and spatial information and less susceptible to various noises, it is suitable for initiating level set evolution. The level set evolution stabilizes automatically once it reaches genuine boundary [9].

## Feature extraction

Feature extraction is an important step for any classification task. In this work, the performance breast cancer detection using four different texture features: Gray Level Co-Occurrence Matrix (GLCM), Gray Level Difference Matrix (GLDM), LAWs texture energy measure and Local Binary Pattern (LBP) were analysed.

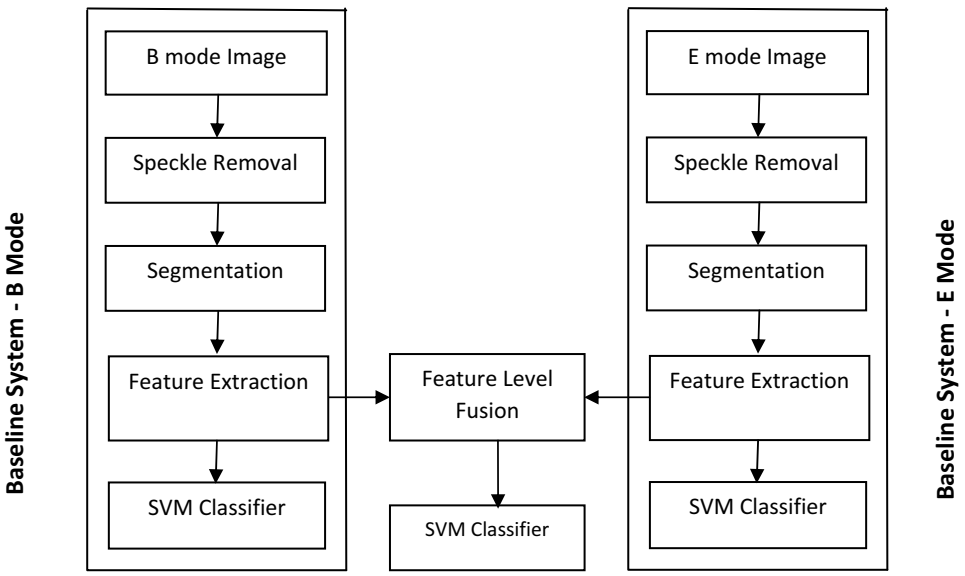


**Fig. 1** Block diagram of the proposed breast cancer detection system

### Gray level co-occurrence matrix

The GLCM gives a relation between the gray level intensity values of neighbouring pixels in matrix form [10]. An element in GLCM gives the relative frequency of two pixel intensities separated by a distance at a particular angle. The Fig. 2 represents the formation of the GLCM of the gray-level (4 levels) image at the distance d = 1 and the direction θ = 0°. Fourteen features defined by Soh et al. are extracted from GLCM matrix.

### Gray level difference method

GLDM method uses the probability distribution function of gray level difference between two nearby pixels $P_\delta(i)$ to compute texture features [11]. Mean, variance, entropy, skewness, Root Mean Square (RMS) and kurtosis were computed from $P_\delta(i)$, measured at 0°, 45°, 90° and 135° directions [12].

### LAWs

Texture energy measures were derived from three simple vectors namely Average L3 = [1, 2, 3], Edges E3 = [− 1,0,1] and Spots S3 = [− 1, 2, − 1]. Five new vectors namely, Edge E5 = [− 1, − 2, 0, 2, 1], Level L5 = [1, 4, 6], Ripples R5 = [1, − 4, 6, − 4, 1], Spots S5 = [− 1, 0, 2, 0, − 1], Waves W5 = [− 1, 2, 0, − 2, − 1] were obtained by using above mentioned three vectors [13]. Then, Law's Masks were derived by the mutual multiplication of the above vectors. After applying the Law's Mask on image, a feature vector describing texture is derived by calculating the statistical parameters mean, variance, entropy, skewness, RMS and kurtosis.

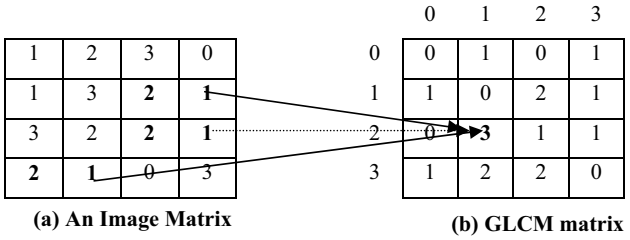


**Fig. 2** **a** An image matrix **b** GLCM matrix

### Local binary patterns

Each pixel in the image is thresholded with the centre value of its 3 × 3 neighbourhood by LBP operator to get a binary result [14, 15]. It is usually applied on gray scale images. The simplest form of LBP is explained below. Consider an example pixel P and its 3 × 3 neighbourhoods as shown in Fig. 3. If the neighbourhood of the centre pixel has larger value than the value of centre pixel value P, then binary 1 is given to that position. Otherwise a binary 0 is given to that position. This process is repeated for all eight neighbours to obtain the binary code for the centre pixel P. Also, the eight neighbours of P are represented with an 8-bit unsigned number.

The final LBP code for the pixel P is obtained by performing sum of element wise multiplication between the binary codes generated and the number representation of the neighbours. Similarly, the LBP codes for all the pixels in the image are formed. The LBP operator with 16 pixel neighbourhood has 65536 ($2^{16}$) different output values and 243 different rotation invariant patterns in the circularly symmetric set of 16 pixels. The two-dimensional histograms of LBP output values are used to quantify these texture descriptors.

## Feature fusion

Selection of an appropriate set of features is an important task for any classification system. The feature fusion is used to generate a new feature set from the selected set of features. The main aim of feature fusion is reduction of features by eliminating redundant information and formation of new discriminant feature set by merging two or more features of different domains to reduce the "curse of dimensionality" problem. The key essence of feature level fusion lies in feature selection process [16].

For selecting optimum sub set of texture features for breast cancer detection, Particle Swarm Optimization (PSO)

**Fig. 3** Original US images of a malignant case

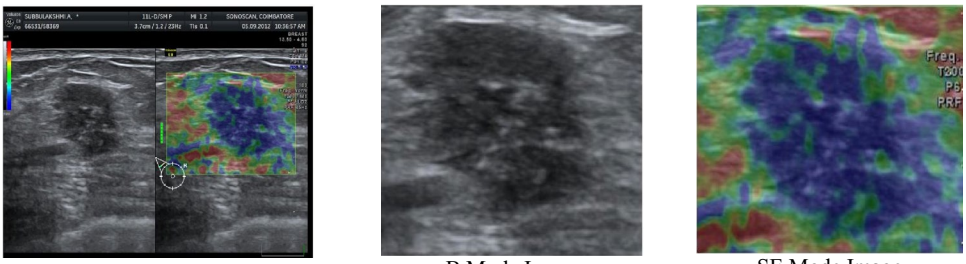

algorithm is used. The classification accuracy obtained from Optimum Path Forest (OPF) classifier is used as a fitness function. The optimum features from B mode and Elastography images are separately selected by PSO based feature selection method and then fused serially to get final feature set for classification.

## Particle swarm optimization

Particle swarm optimization is an optimization algorithm inspired by swarm intelligence of birds and fish, which optimizes a problem by iteratively improving a candidate solution with regard to a given quality measure. It simulates the behaviour of bird flocking. Suppose a group of birds are randomly searching their food in an area where there is only one piece of food available. All the birds do not know where the food is. The best strategy to find the food is to follow the bird which is nearest to the food. This basic strategy is used in PSO to solve the optimization problems. Each single solution in PSO is a bird in the search space, called as particle. Each particle has its own fitness value evaluated by the fitness function to be optimized and associated with a randomized velocity which directs the flying of the particles. The particles fly through the problem space by following the current optimum particles. PSO is initialized with a group of random particles (solutions) and then searches for optima by updating generations [17]. Population size of 20–50 is most common.

Let S be the size of the swarm, each particle 'i' is initialized with random position $X_i$, velocities $V_i$, The best position of individual particle i in the d dimensional space is $p_{best\ id}$ and $g_{best\ id}$ is the best position of the group in d dimension. The objective function $F_i$ is evaluated using the particles positional coordinates as input values. At each time step, velocity of each particle flying toward its $g_{best}$ and $p_{best}$ location is changed and acceleration is weighted by random terms. The position and velocities are adjusted at each time step and the function is evaluated with new coordinates. When the particle discovers a better solution than anyone that it has found previously, it stores the coordinates in the vector $p_{best}$ id.

At time t, the ith particle velocity $V_i(t)$ can be described as $V_i(t)=[V_{i1}(t), V_{i2}(t)\ldots..\ Vid(t)]$, where $V_{id}$ is the velocity of ith particle with respect to the dth dimension. The velocity update is then given by equation

$$V_{id}^{(t+1)} = w\,V_{id}^{(t)} + c_1 rand_1(p_{best\ id}^{(t)} - X_{id}^{(t)}) + c_2 rand_2\left(g_{best\ id}^{(t)} - X_{id}^{(t)}\right) \quad (1)$$

where $V_{id}^{(t)}$ and $X_{id}^{(t)}$ are the velocity and position of particle i, in d dimensional space respectively. $p_{best\ id}^{(t)}$ is the best position of individual i in d dimensional space until generation t; $g_{best\ id}^{(t)}$ is the best position of the group in d dimension until generation t; w is the inertia weight factor controlling the dynamics of flying; $c_1$ is a cognitive parameter which regularizes the step size in the direction of the personal best position of the particle and $c_2$ is a social parameter used to regulate the maximum step service in the direction of the global best particle; $rand_1$ and $rand_2$ are random variables in the range [0,1]. The value of $V_{id}$ is fixed to the range $[-V_{imax}, V_{imax}]$ to reduce the likelihood that the particle might leave the search space.

The accelerating constants c1 and c2 represent the weighting of the stochastic acceleration term that pulls each particle towards $p_{best}$ and $g_{best}$ positions. Low values allow particles to roam far from target regions before being tugged back, while high values result in abrupt movement towards target regions. Usually $c1=c2=2$.

The position of each particle is updated using the new velocity vector for that particle, so that

$$X_{id}^{t+1} = X_{id}^{t} + V_{id}^{t+1} \quad (2)$$

where $X_{id}^{(t+1)}$ is the new position and $X_{id}^{(t)}$ is the previous position and $V_{id}^{(t+1)}$ is the new velocity. In each iteration, each particle is updated by the best values. The first one is the best solution (fitness) achieved by that particle so far known as personal best or $p_{best}$. The second one is the best value obtained so far by any particle in the population (swarm) known as global best or $g_{best}$.

$$\begin{aligned} &{}^{(t)}_{pbestid} \leftarrow X_{id}^{(t+1)}, if\ f(X)_{id}^{(t+1)} < f\ {}^{(t)}_{(pbestid)} \\ &{}^{(t)}_{gbestid} \leftarrow X_{id}^{(t+1)}, if\ f(X)_{id}^{(t+1)} < f\ {}^{(t)}_{(gbestid)} \end{aligned} \quad (3)$$

where f(X) is the objective function to be minimized.

## Optimum path forest classifier

The OPF classifier was developed by extending the concepts of Image Forest Transform (IFT) to general graphs and exploiting the connectivity relations between data samples in a given feature space [18, 19]. OPF is simple, fast, multiclass and parameter independent classifier which can handle some degree of overlapping between classes and does not make any prior assumption about the shapes.

The OPF uses a set of source nodes (prototypes) with any smooth path-cost function and computes optimum paths from a source node to the remaining ones. In OPF, the training set is a graph with nodes as samples; its arcs are defined by some adjacency relation and weighted by the distances between the feature vectors of their corresponding nodes. Any sequence of distinct samples forms a path connecting the terminal nodes and a connectivity function that gives the maximum arc weight. Each path is assigned with a cost. In each class, prototypes are identified such that every sample is assigned to the class of its most strongly connected prototype i.e. the one which offers an optimum-cost path.

Consider a dataset consists of Z1, 2, 3 and 4 as training, learning, evaluating and test sets respectively. The set ⊆ 1 is a set of prototype examples. The OPF classifier creates a discrete optimal partition i.e. an OPF of the feature space by using the IFT algorithm such that any sample ∈ 2 ∪ 3 ∪ 4 can be classified according to this partition. The path-cost function $C_{max}$ is computed as follows:

$$C_{\max} = \begin{cases} 0, \ if \ \ s \in S \\ +\infty. \ otherwise \end{cases} \tag{4}$$

$$C_{\max}(\pi.\langle s,t\rangle) = \max\{C_{\max}(\pi), d(s,t)\} \tag{5}$$

where (, ) is the distance between samples s and t, a path is defined as a sequence of adjacent samples and $C_{max}()$ computes the maximum distance between neighbouring examples in , when is not a trivial path. A path is said to be a trivial path if node s and t are same and its path cost is 0.

The OPF classifier consists of training and a testing phase. Assuming that the training set consists of the samples of all possible classes, the training phase begins with the construction of a complete graph using the training set samples as nodes and prototype computations. The weights of the edges are marked with a dissimilarity function, for example Euclidean distance. The prototypes are defined as nodes of different classes that share an edge. Thus, it is required to find the elements that fall on the boundary of the classes with different labels. For that purpose, a Minimum Spanning Tree (MST) is computed over the original graph and then the connected elements with different labels are marked as prototypes. The MST holds a relation between the nodes; as they will be connected by minimum cost edges, similar samples tend to be strongly connected. After computing the MST, competition process will start between prototypes in order to build the OPF. Once the prototypes are found, the MST is partitioned into a collection of trees by removing the edges between prototypes and setting the associated costs to zero to obtain the OPF. Each tree is rooted in a prototype and all the samples in a given tree belong to the same class. Each node has its associated path cost given by the maximum arc weight in the path to its corresponding prototype. The resulting OPF can be directly used to classify the unknown samples.

In the classification phase, a sample from the test set is taken and it is connected to all training samples. Then, distance from the sample to all training nodes are computed and used to weight the edges. Finally, a cost given by a path-cost function between each training node and the test sample are computed and the training node that offers the minimum path-cost will conquer the test sample. This means that the sample will be classified as belonging to the same class as its more connected prototype. Figure 6 shows various steps involved in training and testing phase of an OPF classifier. In Figure 6, **a** shows the complete graph obtained with edges weighed by dissimilarity, **b** shows the Minimum SpanningTree obtained and the prototypes bounded, **c** shows the optimum-path forest generated at the end of training step of each node and **d** shows the classification process and the identification of associated class of the test the sample.

For feature selection problems using PSO, for each one of the particle, an OPF classifier is trained in 1 and evaluated over 2 in order to assess the fitness value of each particle. Thus, the training and evaluating sets may be different among the particles, since each one of them may encode a different set of features. The main idea is, for each particle in PSO, train OPF over 1 and classify with 2. Therefore, the optimization techniques will be guided by the OPF accuracy over 2 in order to find the most informative set of features. A cross-validation of 10 running is conducted to compute the mean accuracy and standard deviation. To retrieve the most informative features, the following approach is used: A threshold is established in ranges from 10 to 90% and for each value of this threshold, the features that were selected at least a minimum percentage of the running over this learning process in 1 and 2 were marked. For example, a threshold of 40% means, features that were selected by the technique at least 40% of the running have to be chosen. For each threshold, the OPF accuracy was computed over the validating set 3 in order to evaluate the generalization capability of the selected features. Finally, this subset of features were used to train OPF over 1 and to classify the test set 4, which did not participate in any learning process. In this method, 30% of data was employed for training and 20% for learning the most informative set of features, 20% to compose the validating set and the remaining 30% for the test set [20].

## PSO-based feature selection

In this PSO-Based Feature Selection method, the classification accuracy of OPF classifier has been used as the fitness function to find a subset of features that maximize the OPF accuracy over a validation set. The steps involved in method are given below.

*Step 1* Initialize a population of particles with random position and velocities in d dimensional problem space. The population size selected is problem dependent. Population size of 20–50 is most common.

*Step 2* For each particle, evaluate the classification accuracy of OPF classifier as fitness function.

*Step 3* Compare the particle's fitness evaluation with particle's $p_{best}$. If the current value is better than $p_{best}$, then set $p_{best}$ value equal to the current value and the $p_{best}$ location equal to the current location.

*Step 4* Compare fitness evaluation with the population's overall previous best. If current value is better than $g_{best}$, then reset $g_{best}$ to the current particle's array index and value.

*Step 5* At each iteration, update the velocities of all particles according to the Eq. (1).

*Step 6* Between successive iterations, update the positions of all particles according to the Eq. (2).

*Step 7* Repeat Step 2 to Step 6 until a maximum number of iterations is reached. Once terminated, the solution will be obtained as the points of $g(t)_{best\ d}$ and $g(t)_{best\ d}$.

In this method, the particle's position is encoded as binary bit strings of length N, where N is the total number of attributes. Every bit represents an attribute, the value '1' corresponds to selected attribute and '0' corresponds to non-selected attribute. Velocity and position are calculated using Eqs. (1) and (2) and each position is an attribute subset. Then a sigmoid transformation in Eq. (6) is applied on the velocity component to compress the velocities in a range [0, 1].

$$\begin{aligned} S(V_{id}^{new}) &= \frac{1}{1+e^{-V_{id}^{new}}} \\ if(rand < S(V_{id}^{new})),\ then\ X_{id}^{new} &= 1 \\ else\ X_{id}^{new} &= 0 \end{aligned} \tag{6}$$

where: $X_{id}^{new}$ and $V_{id}^{new}$ are the current value and velocity of the dimension d of the individual i.

## Classification

After performing the fusion of echographic and elastographic features, a new feature set is obtained. This new feature set was used to classify the tumours corresponding to the echographic and elastographic image pairs as benign or malignant using Support Vector Machine (SVM) classifier. The confusion matrix was derived from the classification result. Then performance metrics were computed from the confusion matrix.

### SVM classifier

SVM is a supervised technique introduced for a binary classification problem [21]. It creates an optimal separating hyper plane between the classes from the training data and maximizes the margins between two classes of the hyper plane (Steve 1998). In order to maximize the generalization ability and to enhance the classification of non-linear data, the input training data is mapped into a higher dimensional space using kernels. SVM with Radial Bias Function (RBF) kernel is used for classifying the breast images as benign or malignant.

### Performance metrics

There are eight metrics defined in Table 1 have been used for performance evaluation. Accuracy is the percentage of correct classifications of all classes. Classification performance without focusing on a particular class is the most general way of comparing algorithms. It does not favour any particular application. The accuracy does not distinguish between the numbers of correct labels of different classes. Sensitivity and specificity are the two measures that separately estimate a classifier's performance on different classes.

Sensitivity measures the proportion of actual positives which are correctly identified as such and specificity measures the proportion of actual negatives which are correctly identified as negatives.

Precision or positive predictive value is the proportion of actual positive samples in the total number of samples being tested as it is and it might be used to measure exactness of a classifier. A low value of precision indicates a large number of False Positives. Precision and recall are the two measures used to test the efficiency of any test on positive class examples. F1-measure can be used as a single metric to measure the performance of the test for the positive class. It is a composite measure which benefits algorithms with higher sensitivity and challenges algorithms with higher specificity.

For unbalanced class settings, Matthews Correlation Coefficient (MCC) is suitable. MCC value of 1 indicates perfect prediction, −1 shows totally inverse prediction and a value of 0 denotes a random prediction. Balanced Classification Rate (BCR) is more suitable for imbalanced data classes. It shows large value only when both sensitivity and specificity are of large values.

## Results

Since Ultrasound images usually suffer with speckle noise, it is necessary to perform the speckle reduction as a pre-processing step. In pre-processing, the SRAD, which is capable of enhancing and preserving edges, is used for speckle reduction in both B mode and E mode images. The results of pre-processing and segmentation are shown in Figs. 3, 4 and 5. Figure 3 shows the original image of a malignant case and the B mode and SE mode images cropped from this original image. The SRAD output, FLS clustering and segmented mass of B mode image and SE mode image are given in Figs. 4 and 5 respectively.

The performance metrics computed from the classification for the four features are tabulated in Table 2. It is found that, the LBP feature provides accuracy, sensitivity, specificity, precision, F1 score, Mathews Correlation Coefficient and Balanced Classification Rate as 96.2%, 94.4%, 97.4%,

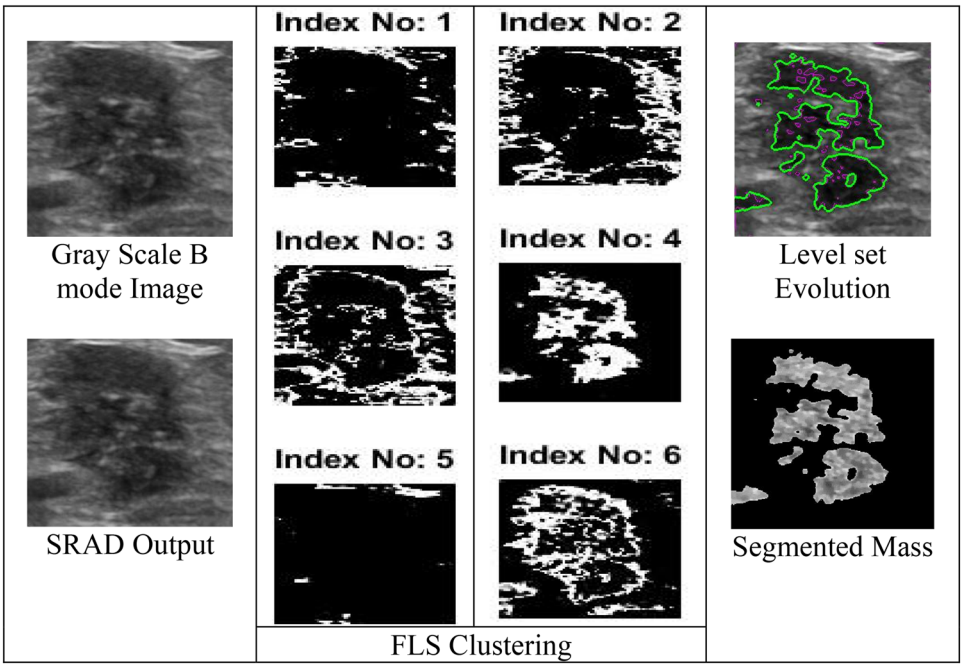


**Fig. 4** SRAD, FLS clustering and segmentation results of B mode image

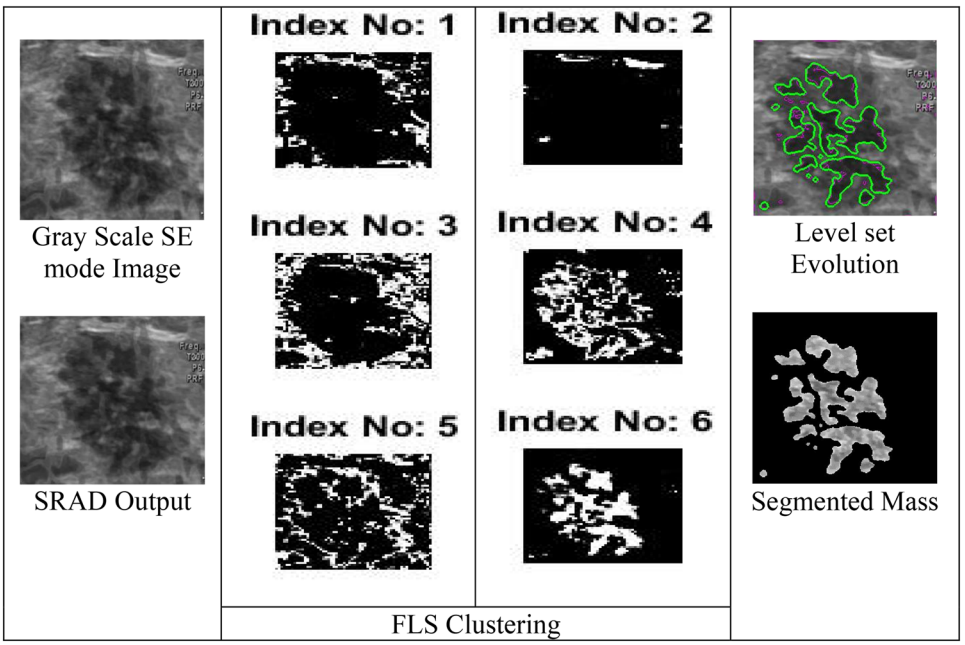


**Fig. 5** SRAD, FLS clustering and segmentation results of SE mode image

96.2%, 95.29%, 0.921, 95.88% respectively, which is better than the performance obtained with the other three features. The maximum values performance metrics obtained are bolded. Although, GLDM feature produces 100% sensitivity, it provides a very low specificity of 89.7%. In case of LBP, a reasonably good sensitivity of 94.4% is obtained with 97.4% specificity. Thus, it minimizes the false positives.

## Discussions

In many literatures, the combined use of more sensitive echographic features and more specific elastographic features were performed and show that it will significantly improve the performance of a breast cancer detection and diagnosis.

Six B mode features (orientation, angularity, undulation, average gradient, gradient & intensity variance) and

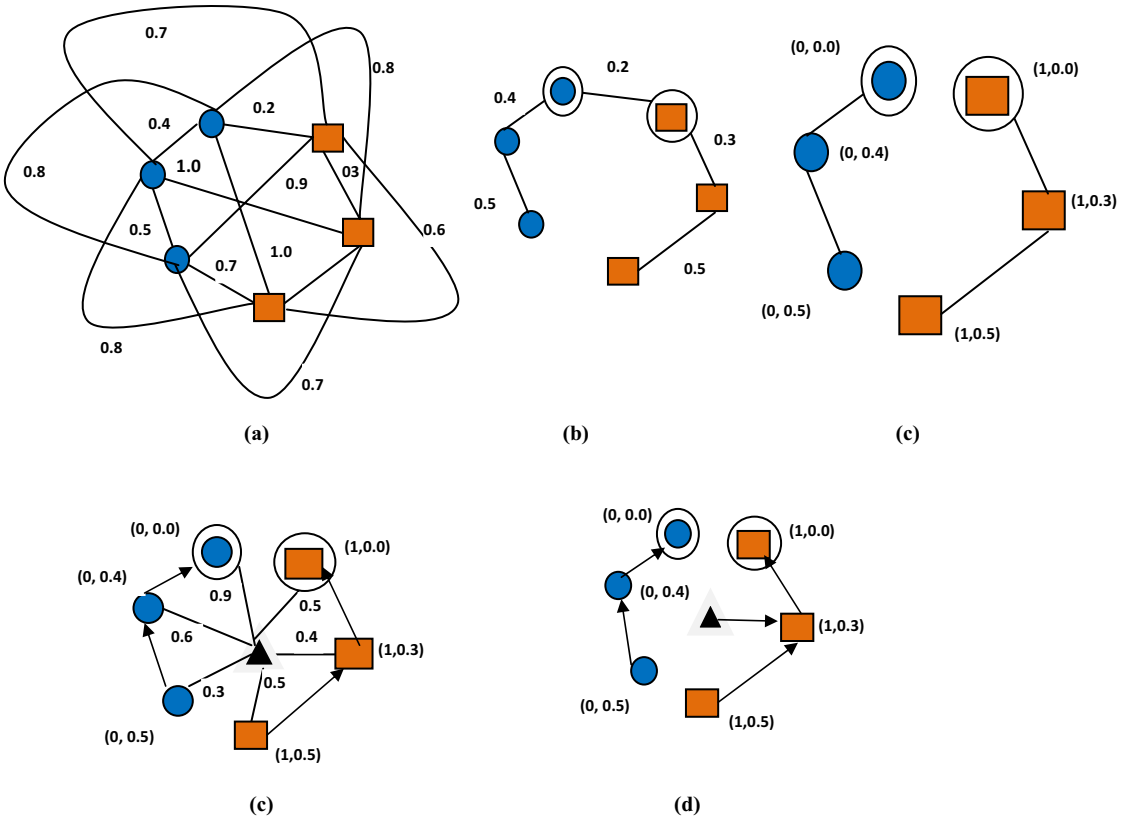


**Fig. 6** Training and testing sequence of the OPF classifier. **a** The complete graph with edges weighed by dissimilarity. **b** The MST and prototypes bounded. **c** Optimum-path forest generated at the end of training step of each node. **d** Classification process and then it is identified that the triangle sample is associated to the class 1 (rectangle)

**Table 1** Performance metrics

| S. no. | Measure | Formula |
|---|---|---|
| 1. | Accuracy | $ACC = \frac{TP+TN}{FP+FN+TP+TN}$ |
| 2. | Sensitivity | $SEN = \frac{TP}{P} = \frac{TP}{FN+TP}$ |
| 3. | Specificity | $SPC = \frac{TN}{N} = \frac{TN}{FP+TN}$ |
| 4. | Precision | $PRE = \frac{TP}{TP+FP}$ |
| 5. | F1score | $F_1 = 2 \times \frac{PRE \times SEN}{PRE + SEN}$ |
| 6. | Matthews correlation coefficient | $MCC = \frac{TP.TN-FP.FN}{\sqrt{(TP+FP)(TP+FN)(TN+FP)(TN+FN)}}$ |
| 7. | Balanced classification rate | $BCR = \sqrt{SEN \times SPC}$ |

*TP* true positive, *TN* true negative, *FN* false negative, *FP* false positive

**Table 2** Performance metrics computed

| Feature | ACC (%) | SEN (%) | SPC (%) | PRE (%) | F1 | MCC | BCR (%) |
|---|---|---|---|---|---|---|---|
| GLCM | 84.1 | 94.4 | 76.9 | 73.9 | 82.90 | 0.703 | 85.20 |
| GLDM | 93.9 | 100 | 89.7 | 87.1 | 93.11 | 0.884 | 94.71 |
| LAW | 92.4 | 88.9 | 94.9 | 92.3 | 90.57 | 0.843 | 91.85 |
| LBP | **96.2** | 94.4 | **97.4** | **96.2** | **95.29** | **0.921** | **95.88** |

five elastographic features (mean, median, mode, strain difference & strain ratio,) were used to classify 181 biopsy proven benign and malignant tumours. The evaluated accuracy, sensitivity, specificity and AUC values were 86.2%, 83.8%, 87.6% and 0.84 respectively for the elastographic features alone and 82.3%, 70.6%, 89.4% and 0.78 respectively with the use of B mode features alone. These metrics were improved to 90.6%, 95.6%, 87.6% and 0.92 respectively, when the elastographic and B mode features were combined for evaluation [22].

The same authors have also proposed another technique wherein the representative slice was automatically chosen based on either the stiffness inside the tumour or the contrast between the tumour and the surrounding normal tissue, then segments the tumour, extracts the B mode and elastographic features from the segmented tumour and evaluates the performance using binary logistic regression model with the leave-one out cross-validation method to classify the tumours as malignant or benign [23]. The performance of the automatically selected slices and physician selected slices were compared separately for the B mode, elastographic and combined B mode and elastographic features. Seventeen B mode US features and four elastographic features such as shape, orientation, margin, lesion boundary, echo pattern, posterior acoustic feature and 11 GLCM texture features were extracted from B mode images and two tumour elasticity features and two lesion boundary elasticity features were extracted from elastography images. The authors showed that improved accuracy was obtained when both the B mode and elastographic features were used to characterize the tumour. The accuracy obtained was 86.1% for the slice based on the stiffness inside the tumour, 90.1% for the slice that contrast between the tumour and the surrounding normal tissue and 89.4% for the physician-selected slice. Also, they have identified that the diagnostic performance of elastographic, B mode, or combined features using automatically selected representative slices is similar to that of slices selected by physicians. Hence they claimed that the automatic selection of representative slice could be used to reduce the observer variability and diagnostic performance could be increased by combining the B mode and elastographic features.

The diagnostic performance of B mode, elastography and combined examinations of axillary node metastasis in breast cancer were compared by calculating the strain ratio of the lymph node and subcutaneous fat tissue. Sensitivity of 87.1% is obtained with combined examination which is better than the sensitivity obtained with independent examination [24].

Sonoelastographic scoring and Strain Ratio (SR) were combined to differentiate 190 breast masses as benign and malignant against the histopathology standard in a prospective study. B mode images were classified according to the BIRADS and the hardness of Sonoelastography image was determined with 5-point Elasticity Score (ES) and SRs of the lesions. There was a significant difference in the mean SRs between benign and malignant masses. The AUC for combination of ES and SR (0.964) was higher than for ES alone (0.852) and B mode US alone (0.823) [25].

A study was conducted to determine whether elastography of axillary Lymph Nodes (LNs) combined with B mode US is capable of differentiating the benign from the metastatic state in 89 female patients with breast cancer. The sensitivity and specificity were 80% and 88% respectively, for B mode US 86% and 90% for elastography alone and 84% and 98% for the combined assessment [26].

Hundred and fourteen solid lesions of 100 consecutive patients were classified by Mammography, B mode and further analyzed with elastography and the results were compared with histopathologic findings. Among these 3 methods, elastography was most specific 95.1% and its accuracy of 81.7% was equal to Mammography (82.5%) but higher than that of B mode (71.9%). The best sensitivity (90.9%) and accuracy (93.8%) were obtained with combination of elastography and B mode [27].

Texture, strain and shape features had been computed from the segmented lesions of B mode and EI and found that some distinct features in EI and increases the specificity [28]. Combination of these features was used with back-propagation neural network for the classification of 62 biopsy proven breast masses. The accuracy, sensitivity and specificity were reported as 82.25, 92.86 and 73.53% [29].

A CAD system for automatic breast mass classification was developed by extracting quantitative strain features from elastographic images. A database with 45 malignant and 45 benign breast masses was used. To highlight stiff tissues with darker values the gray-scale pixels around tumour area on B mode images were classified into white, gray and black by fuzzy c-means clustering. Six quantitative strain features and 15 significant B mode features such as the best-fit ellipse properties and Normalized Radial Length (NRL) features were extracted. The feature set was evaluated by a binary logistic regression model with backward elimination used for feature selection. The accuracy, sensitivity, specificity and AUC obtained for the strain features were 80%, 80%, 80% and 0.84 respectively. Combination of strain features and B mode features produces a significantly better AUC of 0.93 and hence better distinguish malignant tumours from benign tumours [30].

The results obtained from the proposed system shows that the use of LBP feature improves the detection performance significantly. The overall performances achieved in existing CAD using elastographic and echographic features are tabulated in Table 3 and compared with this proposed technique. An improvement of 6.18% in accuracy is achieved compared

**Table 3** Performance comparison of existing works

| Author | Moon et al. [22] | Selvan et al. [29] | Lo et al. [30] | Proposed method |
|---|---|---|---|---|
| Techniques used | 5 elastographic features & 6 B-mode features neural network | Texture, strain and shape features back-propagation neural network | Six quantitative strain features & 15 significant B mode features | LBP feature from B mode & elastographic images PSO based feature fusion SVM |
| Accuracy (%) | 90.6 | 82.25 | 80 | 96.2 |
| Sensitivity (%) | 95.6 | 92.86 | 80 | 94.4 |
| Specificity (%) | 87.6 | 73.53 | 80 | 97.4 |

to that obtained by Moon et al. The specificity is also improved by 11.19%. Though the sensitivity obtained with this proposed technique is less compared to that obtained with Moon et al., the specificity is much higher. This shows that this system could reduce the false positive detection in breast cancer diagnosis.

## Conclusions

Breast cancer detection system using fusion of texture features from ultrasound elastographic and echographic images through PSO is implemented and its performance was studied. Among the four texture features used, LBP provides better performance and it also gives higher accuracy and specificity than those reported in previous literatures. The other performance metrics which were not addressed in previous literatures: precision, F1 score, MCC and BCR were computed and better values were obtained in this work.

Simple LBP is used in this work. It is a nonparametric local texture operator with low computational complexity and has low sensitivity to the changes in illumination. It compares the gray level of a pixel in an image and gray levels of its local neighbourhood pixels and generates a binary pattern code, which best describes the texture present in the tumour and provide better discrimination between the malignant and benign tumours. Hence, the use of LBP produces better performance compared to the other features.

There are some disadvantages faced with simple LBP: (i) its window size is fixed (ii) It neglects the effect of the central pixel in local region (iii) LBP code is rotationally variant (iv) The size of the features increases exponentially with the number of neighbours which leads to an increase of computational complexity in terms of time and space (v) The structural information captured by this LBP is limited (vi) Only pixel difference is used, magnitude information is ignored. There are several variants of LBP discussed in the literature to overcome these limitations. Hence, to achieve further improvements in the detection performance, an elaborate research work might be performed with the variants of LBP.

Serial fusion doubles the dimension of the feature vector when compared to that of feature vector obtained from either echography or elastography image alone. As parallel fusion does not change the dimension of the feature vector, an appropriate method to fuse the features in parallel manner may be researched to reduce the feature dimension.

**Acknowledgements** The authors would like to express their sincere thanks to Dr. Boopathi Vijayaragavan from Sonoscan center for providing ultrasound elastographic and echographic images of benign and malignant breast tumours and guiding in identification of abnormal findings.

## Compliance with ethical standards

**Conflict of Interest** There is no conflict of interest exit in the submission of this manuscript, and the manuscript is approved by all authors for publication.

**Informed consent** Informed consent was obtained from all individual participants included in the study.

## References

1. Raza S, Odulate A, Ong EM, Chikarmane S, Harston CW (2010) Using real-time tissue elastography for breast lesion evaluation. J Ultrasound Med 29(4):551–563
2. Leong LCH, Sim LSJ, Lee YS, Ng FC, Wan CM, Fook-Chong SMC, Tan PH (2010) A prospective study to compare the diagnostic performance of breast elastography versus conventional breast ultrasound. Clin Radiol 65(11):887–894
3. Lee JH, Kim SH, Kang BJ, Choi JJ, Jeong SH, Yim HW, Song BJ (2011) Role and clinical usefulness of elastography in small breast masses. Acad Radiol 18(1):74–80
4. Fu LN, Wang Y, Huang YH (2011) Value of ultrasound elastography in detecting small breast tumors. Chin Med J 124(15):2384–2386
5. Wojcinski S, Dupont J, Schmidt W, Cassel M, Hillemanns P (2012) Real-time ultrasound elastography in 180 axillary lymph nodes: elasticity distribution in healthy lymph nodes and prediction of breast cancer metastases. BMC Med Imaging 12(1):35
6. Youk JH, Son EJ, Gweon HM, Kim H, Park YJ, Kim JA (2014) Comparison of strain and shear wave elastography for the differentiation of benign from malignant breast lesions, combined with B-mode ultrasonography: qualitative and quantitative assessments. Ultrasound Med Biol 40(10):2336–2344

7. Hao SY, Ou B, Li LJ, Peng YL, Wang Y, Liu LS, Parajuly SS (2015) Could ultrasonic elastography help the diagnosis of breast cancer with the usage of sonographic BI-RADS classification? Eur J Radiol 84(12):2492–2500
8. Yu Y, Acton ST (2002) Speckle reducing anisotropic diffusion. IEEE Trans Image Process 11(11):1260–1270
9. Li BN, Chui CK, Chang S, Ong SH (2011) Integrating spatial fuzzy clustering with level set methods for automated medical image segmentation. Comput Biol Med 41(1):1–10
10. Haralick RM, Shanmugam K (1973) Textural features for image classification. IEEE Trans Syst Man Cybern 6:610–621
11. Weszka JS, Dyer CR, Rosenfeld A (1976) A comparative study of texture measures for terrain classification. IEEE Trans Syst Man Cybern 4:269–285
12. Tang J, Rangayyan RM, Xu J, El Naqa I, Yang Y (2009) Computer-aided detection and diagnosis of breast cancer with mammography: recent advances. IEEE Trans Inf Technol Biomed 13(2):236–251
13. Laws KI (1979) Texture energy measures. In: Proceedings of image understanding workshop, pp 47–51
14. Ojala T, Pietikäinen M, Harwood D (1996) A comparative study of texture measures with classification based on featured distributions. Pattern Recognit 29(1):51–59
15. Ojala T, Pietikäinen M, Mäenpää T (2001) A generalized local binary pattern operator for multiresolution gray scale and rotation invariant texture classification. In: International conference on advances in pattern recognition. Springer, Berlin, pp 399–408
16. Mangai UG, Samanta S, Das S, Chowdhury PR (2010) A survey of decision fusion and feature fusion strategies for pattern classification. IETE Tech Rev 27(4):293–307
17. Kennedy J (2011) Particle swarm optimization. In: Encyclopedia of machine learning. Springer, New York, pp 760–766
18. Papa JP, Falcao AX, Suzuki CT (2009) Supervised pattern classification based on optimum-path forest. Int J Imaging Syst Technol 19(2):120–131
19. Papa JP, FalcãO AX, De Albuquerque VHC, Tavares JMR (2012) Efficient supervised optimum-path forest classification for large datasets. Pattern Recognit 45(1):512–520
20. Nakamura RY, Pereira LA, Costa KA, Rodrigues D, Papa JP, Yang XS (2012) BBA: a binary bat algorithm for feature selection. In: 2012 25th SIBGRAPI conference on graphics, patterns and images (SIBGRAPI), pp 291–297. IEEE
21. Boser BE, Guyon IM, Vapnik VN (1992) A training algorithm for optimal margin classifiers. In: Proceedings of the fifth annual workshop on computational learning theory, pp 144–152. ACM
22. Moon WK, Huang CS, Shen WC, Takada E, Chang RF, Joe J, Kobayashi M (2009) Analysis of elastographic and B-mode features at sonoelastography for breast tumor classification. Ultrasound Med Biol 35(11):1794–1802
23. Moon WK, Chang SC, Chang JM, Cho N, Huang CS, Kuo JW, Chang RF (2013) Classification of breast tumors using elastographic and B-mode features: comparison of automatic selection of representative slice and physician-selected slice of images. Ultrasound Med Biol 39(7):1147–1157
24. Choi JJ, Kang BJ, Kim SH, Lee JH, Jeong SH, Yim HW, Jung SS (2011) Role of sonographic elastography in the differential diagnosis of axillary lymph nodes in breast cancer. J Ultrasound Med 30(4):429–436
25. Mousa AE, Aboelatta M, Zalata K (2012) Combined sonoelastographic scoring and strain ratio in evaluation of breast masses. Egyptian J Radiol Nucl Med 43(4):647–656
26. Tsai WC, Lin CKJ, Wei HK, Yu BL, Hung CF, Cheng SH, Chen CM (2013) Sonographic elastography improves the sensitivity and specificity of axilla sampling in breast cancer: a prospective study. Ultrasound Med Biol 39(6):941–949
27. Mohey N, Hassan TA (2014) Value of mammography and combined grey scale ultrasound and ultrasound elastography in the differentiation of solid breast lesions. Egyptian J Radiol Nucl Med 45(1):253–261
28. Selvan S, Kavitha M, Shenbagadevi S, Suresh S (2010) Feature extraction for characterization of breast lesions in ultrasound echography and elastography. J Comput Sci 6(1):67
29. Selvan S, Shenbagadevi S, Suresh S (2015) Computer-aided diagnosis of breast elastography and B-mode ultrasound. In: Artificial intelligence and evolutionary algorithms in engineering systems. Springer, New Delhi, pp 213–223
30. Lo CM, Chang YC, Yang YW, Huang CS, Chang RF (2015) Quantitative breast mass classification based on the integration of B-mode features and strain features in elastography. Comput Biol Med 64:91–100